A Single-Station Automated Earthquake Location System at Wied Dalam Station, Malta

Matthew R. Agius[1] and Pauline Galea[2]

INTRODUCTION

The seismicity of the Sicily Channel, bordered by the Sicilian, Tunisian, and Libyan coastlines, is mainly controlled by active faults of the Sicily Channel rift zone (SCRZ). This region is characterized by a moderate level of earthquake activity with magnitudes generally below 5.0. However, most seismicity, especially south of the Maltese islands, has, to date, either gone unreported or been poorly located owing to difficulties in instrumental coverage. Since many earthquakes are recorded only on a single station on Malta (broadband station WDD), it was deemed necessary to develop a routine procedure for detecting and locating earthquakes using three-component polarization analysis. Such a system, nicknamed LESSLA (Local Earthquake Single-Station Location Analyser) has been successfully implemented since 2005. It uses an automated method of recognizing local/regional events based on a weighting scheme applied to triggers in different sampling streams. LESSLA has allowed a lower detection threshold for earthquakes in the Sicily Channel, and as a result provided new insights into the pattern of seismicity on the rift zone. LESSLA has also had a good success rate at rapidly and accurately reporting larger events as far as the Greek subduction zone. The description, performance, and limitations of the system are here discussed.

GEOLOGICAL SETTING

The Seismic Monitoring and Research Unit (SMRU), University of Malta (Central Mediterranean), has operated a three-component broadband seismic station (WDD) since 1995 as part of the Mediterranean network MedNet, run by the Istituto Nazionale di Geofisica e Vulcanologia (INGV), Rome. Since 2002, WDD has also been a real-time data contributor to the Virtual European Broadband Seismic Network (VEBSN) managed by ORFEUS Data Centre, the Netherlands (van Eck *et al.* 2004). WDD consists of an STS-2 / Quanterra data acquisition system with a maximum sampling frequency of 80 sps. Handling and archiving of data in SEED format, as well as real-time Internet transmission within MedNet and the VEBSN, is done using the SeisComp/SeedLink protocol developed as part of the EC-Project MEREDIAN (EVRI-CT-2000-40007). WDD is the only seismic station on the Maltese islands.

The Maltese islands (total land area of 300 km^2) lie on a relatively stable plateau of the African foreland, the Pelagian Platform, about 200 km south of the convergent segment of the Europe-Africa plate boundary that runs through Sicily (Figure 1). The Pelagian Platform forms a shallow shelf separating the deep Ionian basin from the western Mediterranean. Its seabed topography is characterized mainly by the NW-trending Pantelleria rift, or Sicily Channel rift zone—a system that features three grabens of Miocene–Pliocene age in which the water depth reaches a maximum of around 1,700 m (Reuther and Eisbacher 1985). The grabens are governed by a fault system that extends throughout the Sicily Channel from southern Sicily to Tunisia, and which has also been responsible for the major tectonic and geomorphological development of the Maltese islands (Illies 1981).

Seismicity in the Sicily Channel has generally been considered to be low-level and sparse, within depths generally not exceeding 25 km (http://iside.rm.ingv.it/iside). However, continuous monitoring by WDD has revealed that the level of seismic activity is higher than previously believed and that much of the seismicity, in particular to the south of the Maltese islands, had been going undetected and/or unlocated by neighboring networks. An associated problem is that the seismicity in this region has always suffered from poor epicentral location accuracy, especially in the case of earthquakes occurring south of the Maltese islands. This is due to inadequate network coverage, especially before the 1980s, as well as the generally small magnitude of the events. A single-station location procedure at WDD was developed with this problem in mind, in an effort to obtain a more accurate picture of local seismicity.

SINGLE-STATION LOCATION

Most single-station location methods use some form of polarization analysis, although pattern-recognition methods from the field of artificial intelligence have also been proposed (*e.g.*, MacBeth and Dai 1996; Zhizhin *et al.* 2006). A review of single-station location methods and their effectiveness in source parameter estimation is given by Frohlich and Pulliam (1999), who emphasize the need for better global monitoring of events down to magnitude 3.0 in the scenario of the Comprehensive Nuclear-Test-Ban Treaty (CTBT), such coverage being diffi-

1. Dublin Institute for Advanced Studies, School of Cosmic Physics, Geophysics Section, 5 Merrion Square, Dublin 2, Ireland
2. Physics Department, University of Malta, Msida 2080, Malta

doi: 10.1785/gssrl.82.4.545

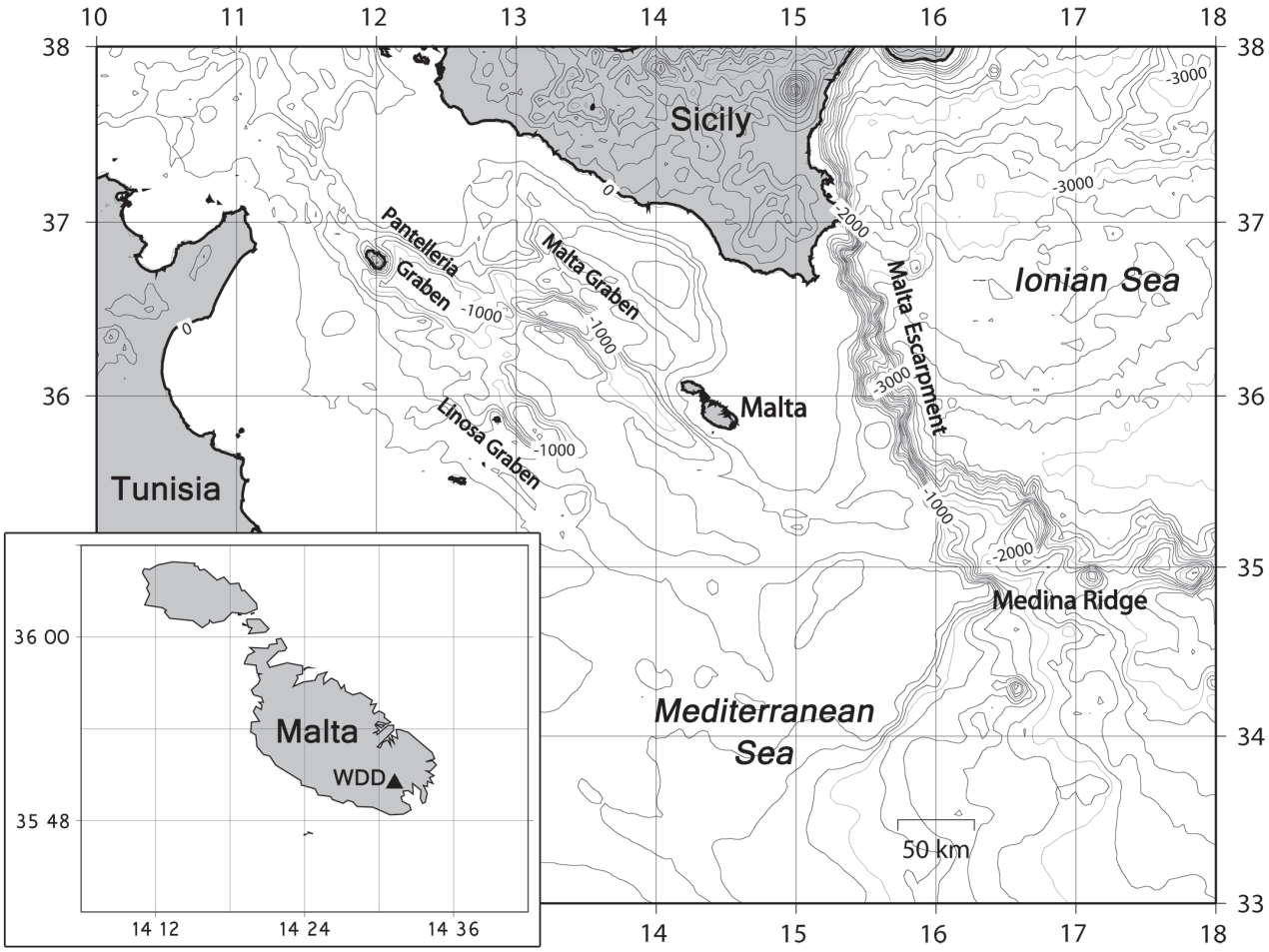

▲ **Figure 1.** Bathymetry of the Sicily Channel and position of the Maltese islands. Inset shows the location of station WDD.

cult to achieve using conventional network locations based on travel times.

Most often, polarization analysis involves the construction of a data covariance matrix from the three-component broadband signal, from which the largest eigenvalue yields the eigenvector corresponding to the back-azimuth. The main contributors to these methods were Magotra *et al.* (1987), who used only horizontal channels, and Park *et al.* (1987), Jurkevics (1988), Ruud *et al.* (1988), Ruud and Husebye (1992), and Kim and Gao (1997), who used all three components. Roberts *et al.* (1989) avoided the use of covariance matrix inversion by using auto- and cross-correlation functions of the three orthogonal components within short time-windows, thereby making the processing more computationally efficient. This approach has been used in the present system and will be discussed further on. Ruud and Husebye (1992) further developed an automated detector and seismic bulletin generator based on single-station location that also distinguished between teleseismic and local/regional events by matching apparent velocities to specific frequency ranges.

Event distance is usually estimated from phase identification and separation, or from estimates of the slowness vector in conjunction with travel-time tables. The use of intermediate phases may involve synthetic seismogram modeling (*e.g.*, Dreger and Helmberger 1990, 1993; Zhao and Helmberger 1991). These techniques require good knowledge of the regional crustal structure. More recently, Lockmann and Allen (2005) tested a procedure in which event distance and magnitude are rapidly estimated from the first few seconds of the *P* wave. The hypocentral distance is found by developing a scaling relationship between distance, *P*-wave amplitude, and the predominant period of the *P* wave. This method was adopted in the context of earthquake early-warning using a single station.

Single-station location of local and regional earthquakes is known to be potentially difficult, especially with regard to the back-azimuth estimation. When the signal-to-noise ratio (SNR) is low, high-frequency, near-receiver scattering effects may interfere with the *P*-wave polarization, and filtering out the noise is often difficult. High regional variability in earthquake waveforms also means that single-station analyses in general may have to be "tailored" to the particular station or source region. Where seismograms do not show clear *P* and *S* arrivals, distance calculation based on phase identification may be unreliable. Nonetheless, where no other means of earthquake location is available, and especially where the principal motive is the broad evaluation of the seismicity level of a region rather than very precise location, then the method is a highly useful complement to the conventional seismicity coverage of better monitored areas, and is definitely worth implementing.

LESSLA (Local Earthquake Single-Station Location Analyser)

The requirements for the system to be developed were that it should:

- be fully automated in event detection and processing;
- be able to distinguish local and regional events from teleseismic ones;
- pick the *P* and *S* phases as accurately as possible for the eventual calculation of distance;
- calculate event back-azimuth along a moving time-window in a computationally efficient manner;
- locate and map the events;
- be fully accessible and operable through a Web interface; and
- allow users to judge the automated processing and modify as necessary.

The detailed description of the algorithm is found in Agius (2007). LESSLA is based on the novel idea of utilizing signal characteristics and information contained in the three components of each of three different sampling streams—80 sps (HH), 20 sps (BH), and 1 sps (LH)—for event type recognition, phase identification, and optimum back-azimuth estimation. At present LESSLA performs analysis of a whole 24-hour SEED file (HH, BH, and LH streams) at a scheduled time each night. It is intended to convert to near real-time processing in the future.

LESSLA first filters all nine components using Seismic Analysis Code (SAC). The frequency content of the signals is in part related to whether the earthquake is close or far, and this is reflected in the importance of the different sampling streams. The Nyquist frequency restricts the frequency range observable in a given stream. The filtering used was thus optimized for the different sampling streams. For the LH stream (Nyquist 0.5 Hz) a 0.05–0.10 Hz bandpass was found to best preserve the signal of interest. The BH stream (Nyquist 10 Hz) was high-pass filtered above 0.5 Hz to eliminate unwanted lower frequencies. For the HH stream (Nyquist 40 Hz) a high-pass filter with a 2.5 Hz cutoff was found optimal for suppressing seismic noise.

After filtering, LESSLA "runs through" each component to set up a "day events list." As each trace is processed through time, the standard short-term average/long-term average (STA/LTA) ratio using the power characteristic function (Kanasewich 1981) is compared to trigger and detrigger thresholds to form events. The start of an event is defined as the last minimum point before the sharp increase in the STA/LTA function and the end of the event is either when the STA/LTA gets below a detrigger threshold or when an unrealistically long time has exceeded a duration limit based on the maximum amplitude within the same event. Each stream has a specific configuration for filtering, STA/LTA time windows, and trigger/detrigger thresholds. In principle, events from LH components have a longer time-span as the variation of the STA/LTA is gradual. After the algorithm processes each of the nine channel components in sequence, a list of "events" is generated, each corresponding to a triggered/detriggered segment. A scheme was developed by which events in all or some of the components whose start and end times fall within the same interval are merged and declared as a single event. The start and end time of the single event are taken to be the earliest and the latest time from all the individual component events. The linked list of events now represents the activity of a whole day. Figure 2 shows how matched and overlapped triggered events form a single event.

Recognizing Local/Regional Events

The aim of LESSLA was to process local/regional events, especially those in the Sicily Channel which were being "ignored" by routine processing of neighboring networks. The system thus had to be tailored to carry out this processing as efficiently as possible. Based on the observational experience that local events generally trigger predominantly the HH and/or BH streams, a channel weighting scheme was set up using this criterion to decide whether an event was to be processed further.

The event is assigned a weight of one for each triggered LH component, two for each triggered BH component, and three for each HH component. If all channel components are triggered, the event will have a maximum vote of 18. After looking at possible triggering scenarios, an optimal threshold vote of 11 was chosen to discriminate between events of interest or otherwise. Thus, for example, an event that triggers all HH components and one BH component will be accepted, but one that triggers all BH and one HH component will not. This scheme effectively eliminates teleseismic events and spurious noise events that trigger an unlikely combination of streams, while ensuring that all "true" local/regional events are flagged for further processing and more accurate phase picking.

At the same time, in order to make sure that no event of possible importance is missed, a minimum voting threshold of four labels the event as "possible," and it is then just listed in the daily report with no further processing, allowing the analyst to examine the traces if required. Most teleseismic events fall within this category, and are labeled as such.

Once the begin- and end-time of a listed event is set, a preliminary event classification can be made. Considering the waveform shape of local events, the time difference between the maximum horizontal amplitude and the event begin-time acts like a rough *S-P* calculation, and the event is preliminarily classified as near (< 5 s), local (5–60 s) or regional (60–150 s). These large time differences are required because in most cases the start of the event is influenced by the gradual increase of the STA/LTA in the LH stream and the largest amplitude in the seismogram is likely to be some time after the *S* arrival. This rough classification serves to determine the time-windows to be used in the subsequent processing.

P and *S* Picking

LESSLA now considers each flagged event and reprocesses it from the begin-time to the end-time, using tighter and more sensitive STA/LTA time-windows depending on the preliminary event classification and the respective stream. The correct picking of both the *P* and the *S* phase is critical to the (automated) method since it is the basis of calculating epicentral distance. The algorithm was designed to work best with waveforms typical of local/regional events in the region of interest,

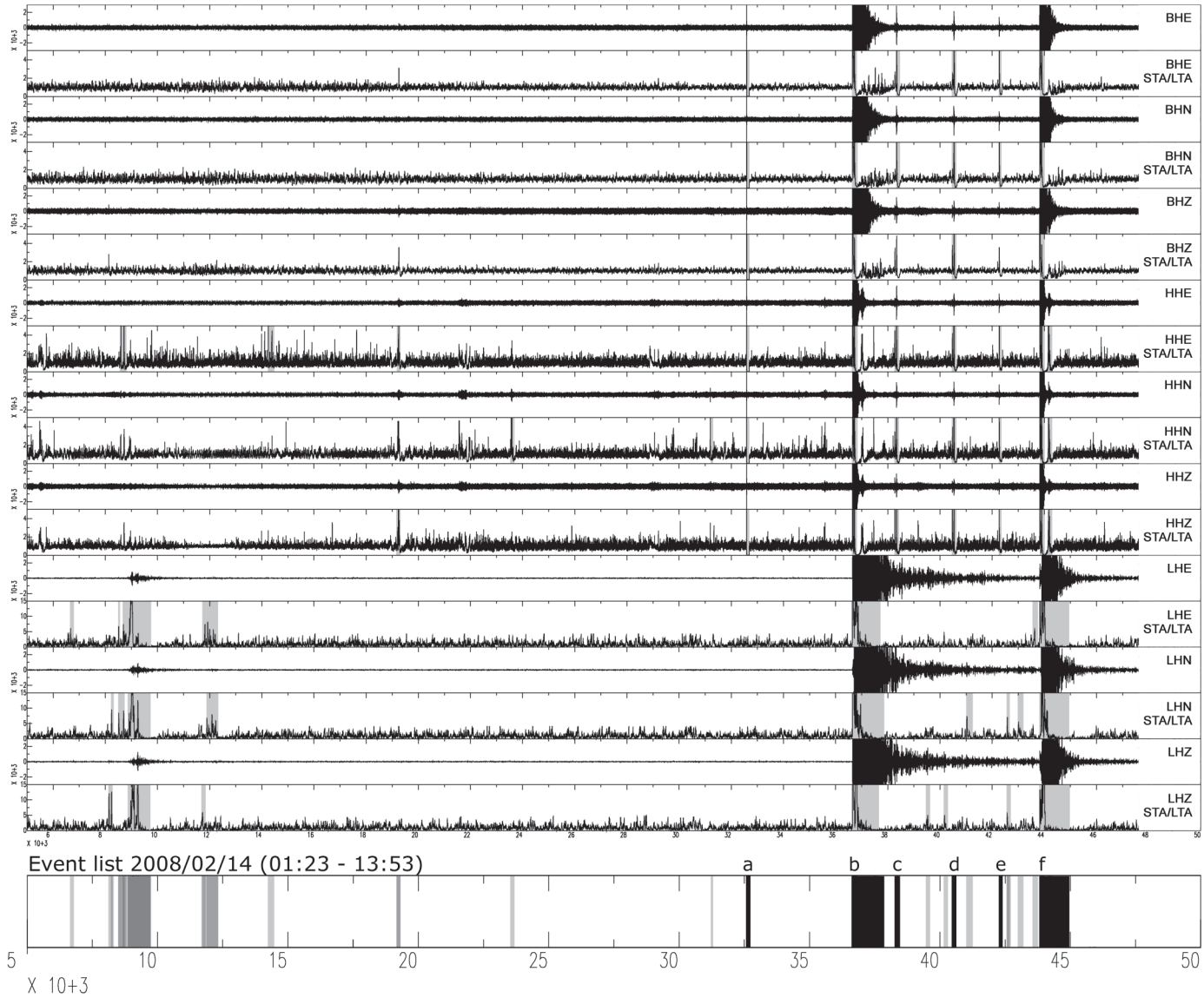

▲ **Figure 2.** Generation of a day event list, using triggers from all the nine streams. The traces show a 12-hour segment for February 14, 2008, which recorded an M_w 6.9 earthquake (Greece, 10:09). Below each component (BHE, BHN, BHZ, HHE, HHN, HHZ, LHE, LHN, LHZ) is the corresponding STA/LTA. The *y*-scale is exaggerated to enable detailed viewing. Triggered/detriggered sections (STA/LTA ≥ 5) are shaded gray. The collective triggers are illustrated at the bottom bar and show the event list of the day. Many LH triggered events are left unprocessed as the sum of weights does not reach the desired criteria; thus the early LH triggered event is disregarded (see section "Recognizing Local/Regional Events"). Only black shaded events are processed further: a) a blast detected in the BH and HH components at 09:03; b) Greece earthquake, notice the variation of the signal content at the different streams, the immediate detrigger for HH and BH, and how LH encapsulates all triggers; c–e) a series of aftershocks detected in BH and HH but not LH mainly due to coda from the mainshock; f) a strong aftershock with characteristics similar to b.

which usually have a very recognizable *S*-onset. In general, a number of picks besides the *P* and *S* phases are present in the seismogram, and the algorithm is designed to detect these by using the STA/LTA ratio. The arrival of a phase is usually characterized by a peak in the STA/LTA function. The algorithm continuously computes the ratio of the current STA/LTA value to the previous STA/LTA minimum, and compares this ratio to a threshold value. If the ratio exceeds this threshold a new "pick" is registered. The time of the previous minimum is taken to be the pick time (Figure 3). This method is similar to Chen's ratio of after-time-average (ATA) to before-time-average (BTA) (Chen 2005), although Chen uses the ratio as an event-trigger algorithm. The method is here referred to as STA/LTA peak/trough algorithm. Safeguards, such as smoothing, amplitude sensitive threshold, and ignoring STA/LTA values less than one are incorporated in the algorithm to ensure that only the most significant picks are triggered.

The procedure is run over all the nine components and a list of picks is generated for the event. The picks are then grouped into clusters based on the time difference between

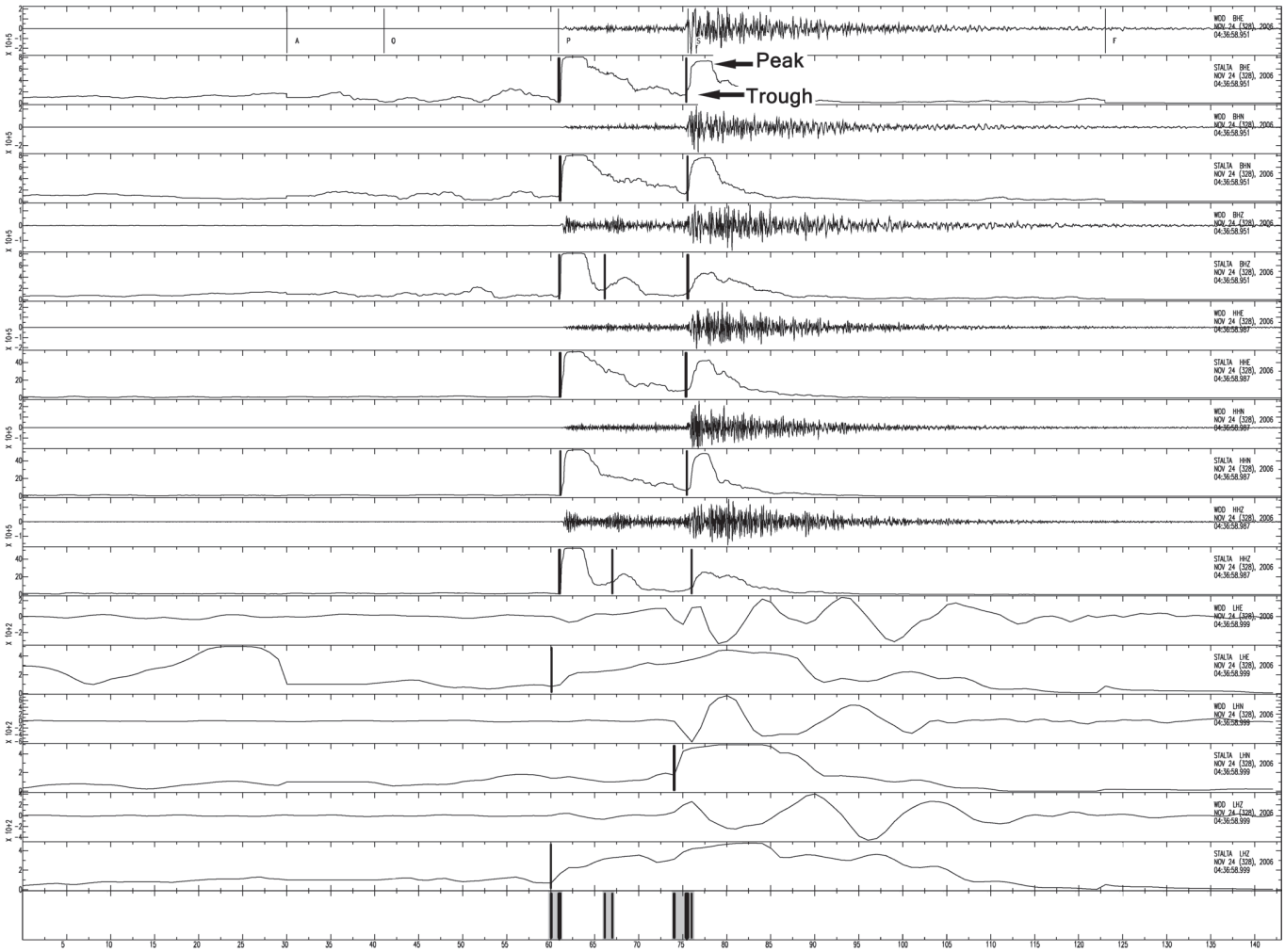

▲ **Figure 3.** Nine-component data of a regional event and corresponding STA/LTA plots. Sequence of plots as in Figure 2. More sensitive STA/LTA time windows are used between A and F. Picks (thick black lines) are generated when the ratio of an STA/LTA peak and preceding trough exceeds a threshold. The collective picks are illustrated in the bottom bar and grouped together in clusters (gray-shaded area). The two clusters with the highest grades are selected for the *P* and *S* pick. The intermediate cluster is likely to represent the arrival of some other phase. The final calculated picks are shown in the top trace. *O* is the calculated origin time.

them (Figure 3). This is similar to what is done in pattern-recognition techniques in artificial intelligence. The cluster range definition varies according to whether the preliminary event classification is near, local, or regional, since the closer the event, the closer together the phases will be. With each pick added to the cluster, the range expands slightly to allow for nearby picks to be included. Each pick is attributed a weight based on which stream it belongs to (HH = 5, BH = 3, LH = 1). The summation of weights within a cluster will be the final grade for that cluster. Picks originating from the HH stream are given the highest weighting so as to prioritize local and regional events. The seismogram can now be represented as a set of clusters rather than a list of picks (Figure 3, bottom bar). The pick time is defined as the average within the cluster. Important seismic phases are distinguished by clusters having the highest grades. For local/regional earthquakes, the *P* and *S* phases are likely to dominate in the seismogram and are usually the two highest graded clusters. LESSLA declares the *P* pick to be the cluster closest to the event start, and the *S* pick the cluster closest to the maximum horizontal amplitude. The *S-P* time interval is now more precisely determined and forms the basis of classifying the events into near ($S\text{-}P < 4$ s), local (4 s < $S\text{-}P$ < 15 s), or regional (15 s < $S\text{-}P$ < 120 s), these categories being somewhat different from the standard definitions of local and regional earthquakes but more meaningful in the local context.

Distance and Origin Time Calculation

The event distance is calculated by making use of a purposely constructed calibration curve of *S-P* time interval against epicentral distance in kilometers, using a dataset of well-located earthquakes that were also recorded on WDD. The locations were obtained from the Euro-Mediterranean Seismological Centre (EMSC) bulletin (http://www.emsc-csem.org) or the INGV bulletin (http://iside.rm.ingv.it). A problem exists with near events ($S\text{-}P < 4$ s) since these are, in the main, quarry blasts, and therefore surface sources. The calibration graph is then not

suitable. In this case, the *S-P* time is provisionally multiplied by a factor of 2.5, following Agius (2003), but a more accurate method for locating such sources is still to be developed. Origin times are estimated using a similar method to the above, using a calibration graph of *P* travel time versus *S-P* time.

Back-Azimuth Calculation

The most sensitive aspect of the procedure is the back-azimuth calculation, especially for high-frequency signals that are more affected by scattering of waves close to the receiver. In order to economize on computation time (remembering that LESSLA works on three different sampling streams), we have chosen to use the algorithm of Roberts *et al.* (1989), which does not involve matrix inversions. The algorithm essentially considers the waveform as made up of the sum of seismic signal, correlated noise on the horizontal components, and random noise, thus:

$$y_n(t) = aP(t) + Q(t) + N_n(t)$$
$$y_e(t) = bP(t) + cQ(t) + N_e(t)$$
$$y_z(t) = P(t) + N_z(t)$$

where $y(t)$ is the observed particle motion, $P(t)$ is the *P*-wave signal, $Q(t)$ is correlated noise on the horizontal components, such as cultural noise, $N(t)$ represents random noise, and a, b, c are real coefficients. By forming the cross powers over a time window of length T, the noise terms are effectively suppressed, thus:

$$E(\langle y_n y_z \rangle) = E(a\langle P^2 \rangle)$$
$$E(\langle y_e y_z \rangle) = E(b\langle P^2 \rangle)$$

so that the back-azimuth is obtained by

$$\tan(az) = \frac{-\langle y_e y_z \rangle}{-\langle y_n y_z \rangle} = \frac{-b}{-a}$$

and there is no 180° ambiguity in the azimuth.

In this paper, the authors define the *predicted coherence C* to be

$$C = 1 - \frac{\langle (y_z - Ay_n - By_e)^2 \rangle}{\langle y_z y_z \rangle}$$

where $(y_z - Ay_n - By_e)$ is effectively a noise term. C is a measure of the degree of linear polarization of the signal and is equal to 1 for a noise-free, linearly polarized signal. The authors use C as a "trigger" parameter to detect an incoming *P*, while in LESSLA, C is used as an additional tool for manual pick confirmation and for making a more reliable judgment about azimuth stability. Roberts *et al.* (1989) also evaluate incidence angles for teleseismic event location. While LESSLA does evaluate the angle of incidence, this feature is not presently used in the case of regional/local event locations.

In LESSLA, the back-azimuth and predictive coherence are calculated continuously within the selected events, for all three streams HH, BH, and LH, using appropriate time-windows and time-steps for each stream. In practice, the back-azimuths for the different streams will in general differ. In the fully automated mode, LESSLA is programmed to select the back-azimuth value following the *P* pick in the HH and BH streams in which the azimuth remains stable for the longer time (that is, the time period during which the azimuth variation is within a predefined range). The mean of the azimuth value over the "stable" period is calculated. The LH back-azimuth proves to be very reliable for more distant earthquakes where the lower frequencies prevail, but is normally beyond the purpose of LESSLA.

When the event distance and back-azimuth from the station have been calculated, the epicenter is located using a spherical earth approximation and plotted. The output of LESSLA is demonstrated in Figure 4, using the example of an event in Greece (2008/02/14 10:09, M_w 6.9). The fully automated *P* and *S* picks, back-azimuth plots, and predictive coherence plots are shown. Note the consistency in the back-azimuth throughout the *P* coda in the BH stream, and the sharp coherence peak at the *P* onset. Although the back-azimuth on the HH stream is much more unstable, a sharp change in the value can still be picked out corresponding to the *P* arrival. In this case, the algorithm rightly chose the BH back-azimuth of 79.89°, which gives an epicentral solution very close to that of EMSC (inset). While Roberts *et al.* (1989) use the predictive coherence as a trigger for picking the *P* onset, the function is here used as a visual criterion for checking the accuracy of *P* and *S* picks, and may be particularly useful when visual, as well as automated, phase picking is difficult. As an example, Figure 5 shows the analysis for the L'Aquila earthquake, Italy (2009/04/06 01:32 M_w 6.2). The automatic picking in this case failed completely for both *P* and *S*, due to a noisy start and unidentifiable *S*, even visually. However, both the *P* and the *S* arrival could be accurately picked (using manual mode, described in the following section) using a combined judgment of changes in back-azimuth and coherence. The back-azimuth change and coherence at the *P* onset are well defined. Again note the stability in the back-azimuth function after the initial *P*. The *S* phase was picked manually using the LH stream, but the change in azimuth and the coherence peak in the BH stream corresponding to this phase give increased confidence to the pick. As a result, the final location was excellent, as seen in the inset.

Figure 6 is an example of a smaller earthquake at a distance of 33 km from WDD (2009/05/02 09:27 M_L 2.9). Note that in this case the LH stream carries no useful information and has not been plotted. The *P* coherence peaks are clear in both BH and HH streams, while the back-azimuth values are close. The algorithm in this case chooses the HH back-azimuth. The inset compares the automated location with that given by INGV.

The back-azimuth plot is also a useful tool that serves to distinguish certain cultural noise from seismic signal, where the cultural noise often presents sustained values of back-azimuth and coherence levels. Figure 7 shows the HH stream of an "event" that at first sight might be interpreted as an earthquake.

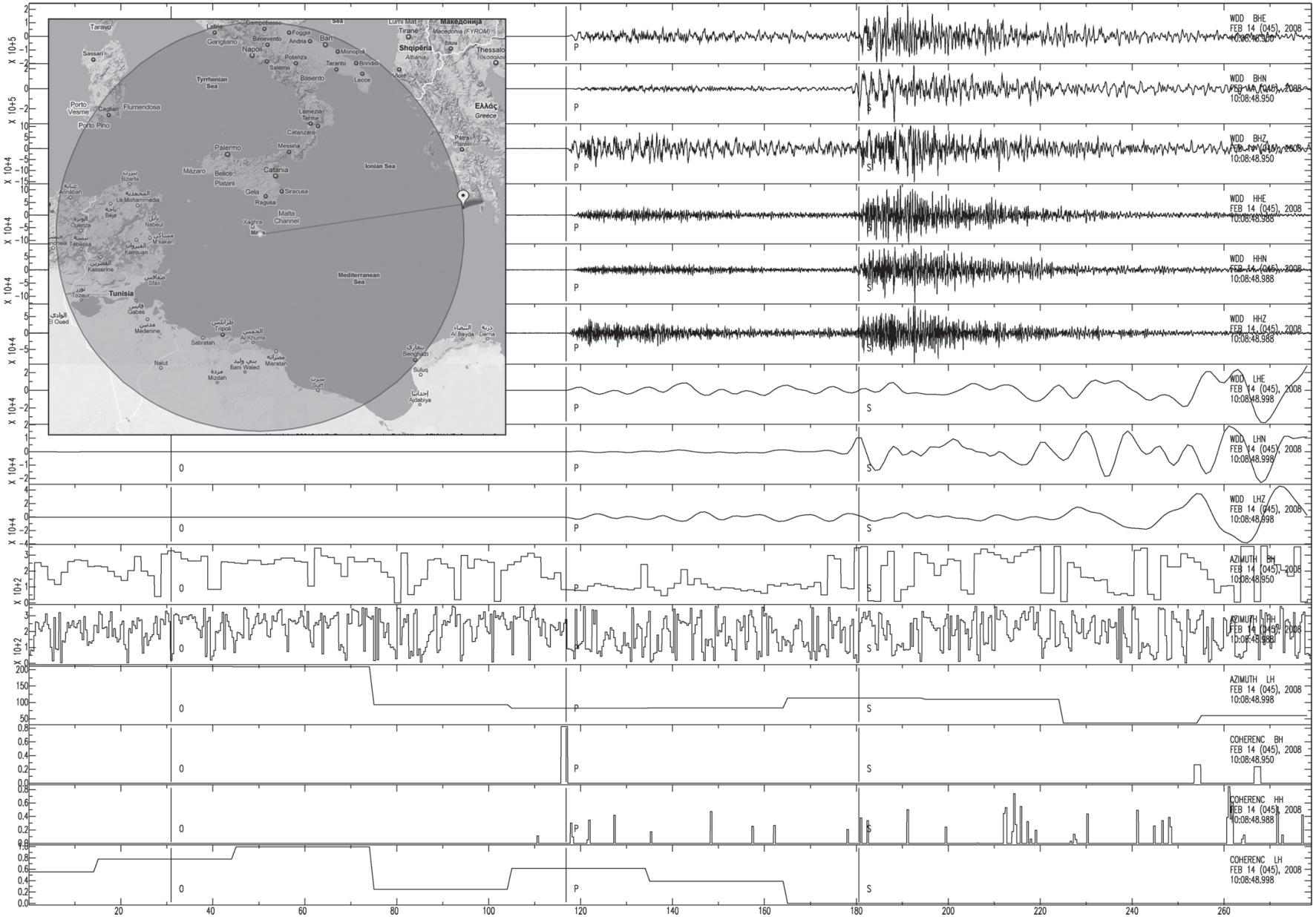

▲ **Figure 4.** LESSLA output, showing fully automated phase picking for all streams, back-azimuth, and coherence functions. (Greece, 2008/02/14 10:09 M_w 6.9). The scale on the back-azimuth plots goes from 0 to 360°. Note the relative stability of the back-azimuth between the *P* and *S* arrivals in the BH stream. The system in this case selected the BH azimuth (79.89°) as the most stable one. Inset: Comparison of the LESSLA and EMSC locations. The marker denotes the EMSC location, the circle shows the radial distance from WDD, and the line points to the LESSLA location.

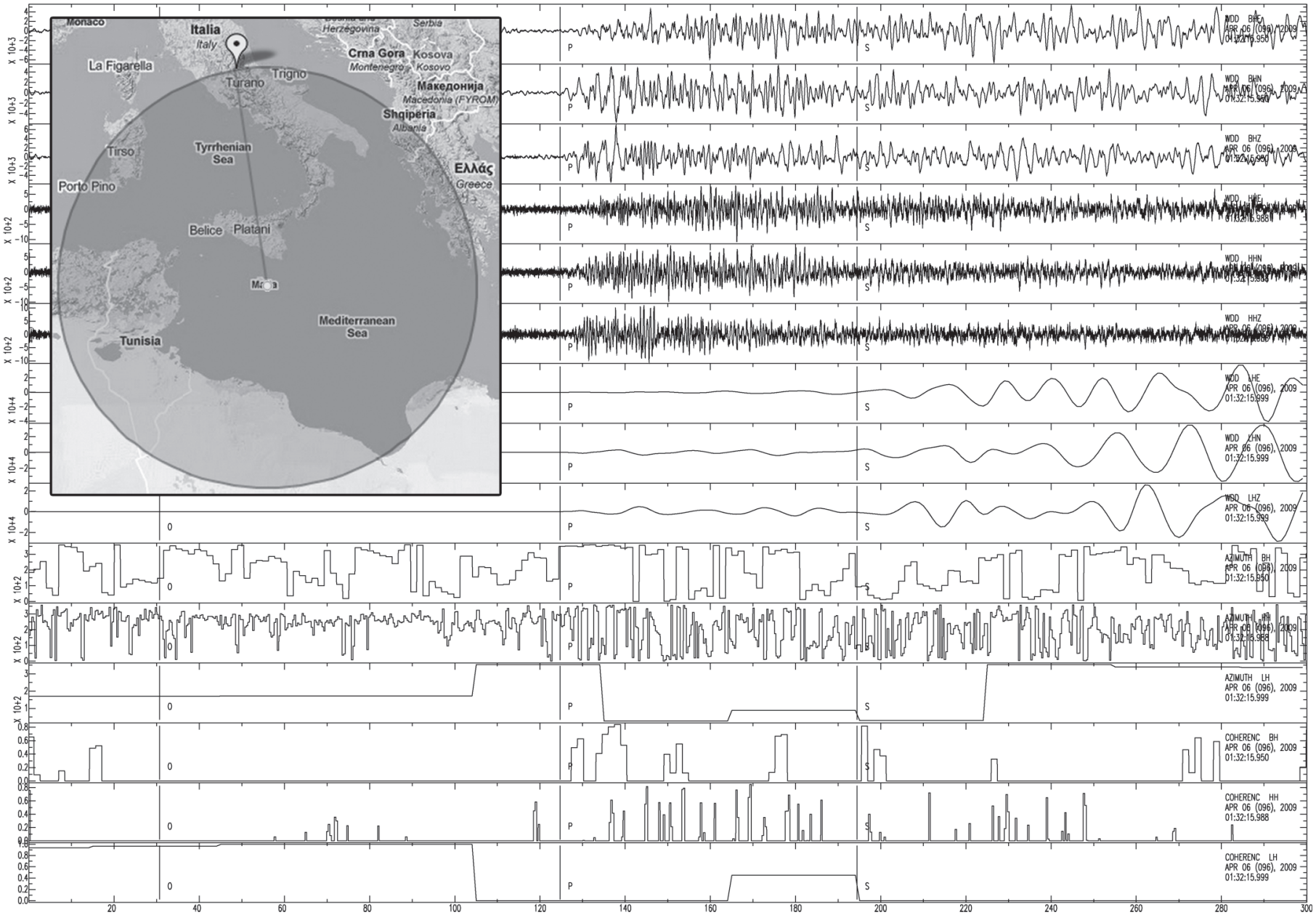

▲ **Figure 5.** Analysis of the L'Aquila earthquake seismogram at WDD (2009/04/06 01:32 M_w 6.2) showing the coherence peak and change of azimuth in the BH stream corresponding to the *S* arrival. Inset: Comparison of LESSLA and EMSC locations, as in Figure 4.

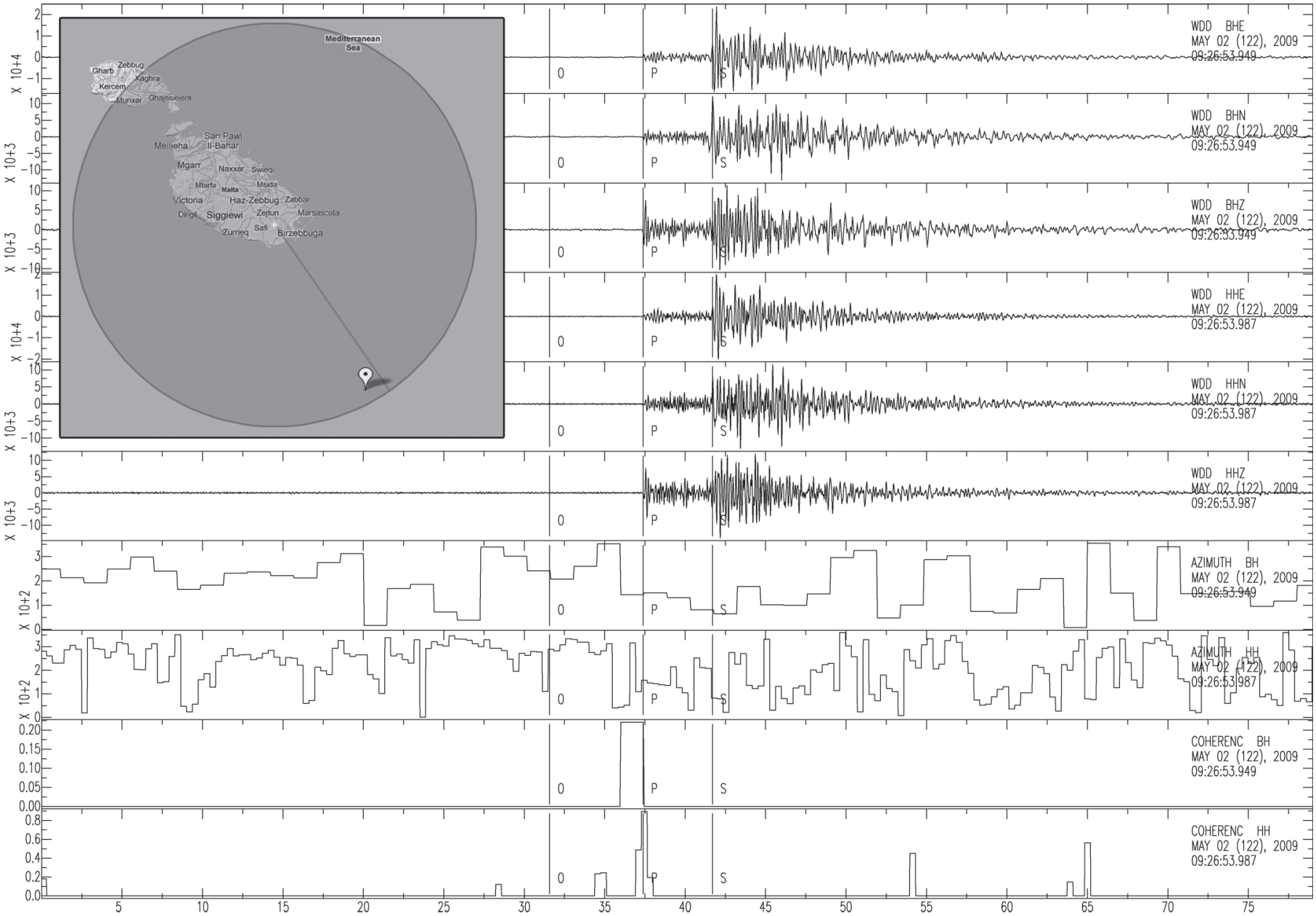

▲ **Figure 6.** A small local earthquake (2009/05/02 09:27 M_L 2.9) at a distance of 33 km from WDD and comparison of location with that of INGV (inset). Note clear coherence peaks at *P* arrival in BH and HH streams.

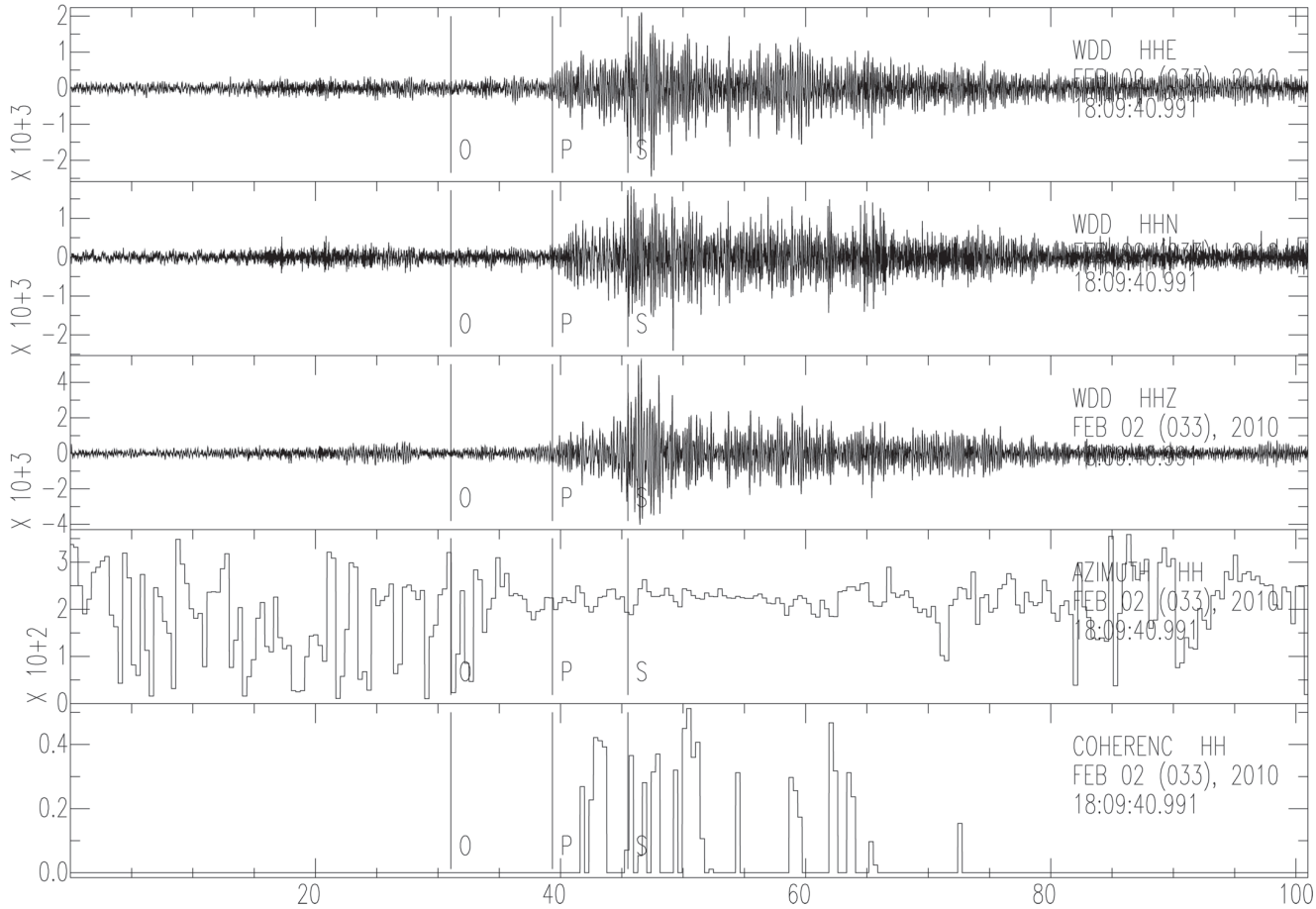

▲ **Figure 7.** Example of the use of azimuth and coherence functions to distinguish between a seismic event and noise. Note the consistency of the back-azimuth, with no change at the *S* arrival.

The system in fact picked acceptable "*P* and *S* phases." However the constant azimuth throughout the waveform, and the persistent coherence, strongly suggests that it consists of cultural noise.

Magnitudes and Bulletin Generation

The maximum horizontal amplitude of the waveform is recorded and used in the calculation of local magnitude M_L, whereas the end of signal phase *F* (Fini) (where the STA/LTA detriggers) is used to calculate the duration magnitude. A complete daily analysis report is generated and sent as an e-mail. The report contains all the parameters relevant to the processing of each event and includes plots of seismograms and analysis in PDF format and a location map. The processed events, as well as those marked as "possible" earthquakes, are added to a database.

Manual Analysis Review

The event database, as well as full manual review of all events, is fully accessible through a Web interface (Figure 8). An event in the database can be viewed in the "Event Window," where a number of tools are available for judging the accuracy of the automated solution and modifying it if necessary. All or any of the nine traces may be viewed on a SeisGram2K Java applet window (http://alomax.free.fr/seisgram/SeisGram2K.html) and the *P* and *S* phases may be manually repicked if necessary. This automatically recalculates the *S-P* time, distance, and origin time, and repositions the picks in the "Analysis" window so that the azimuth at the new *P* arrival is shown for each of the three streams. At this point several factors contribute toward making the best judgment of which azimuth to choose. Besides the stability of the azimuth immediately after *P*, the decision is aided also by consideration of which streams were triggered, which stream exhibits the larger coherence, and which stream appears to display the higher sensitivity, *i.e.*, a sharper change in the azimuth function at the *P* onset. A quality factor from A to C is assigned by the analyst based on a subjective level of confidence in the solution. Quality A is assigned when the *P* and *S* picks are very clear and there is a high level of consistency in the back-azimuth value among the streams.

Multi-Station Location

SeisComP/SeedLink makes it possible to acquire real-time data from other accessible stations. The SMRU receives data from stations in neighboring countries and runs LESSLA on selected stations; however, the analysis of data from another station should strictly only be carried out after proper configuration, especially regarding the *S-P*/distance calibration.

A simple yet highly effective and rapid tool is the "multi-station" location based on the basic "method of circles." When

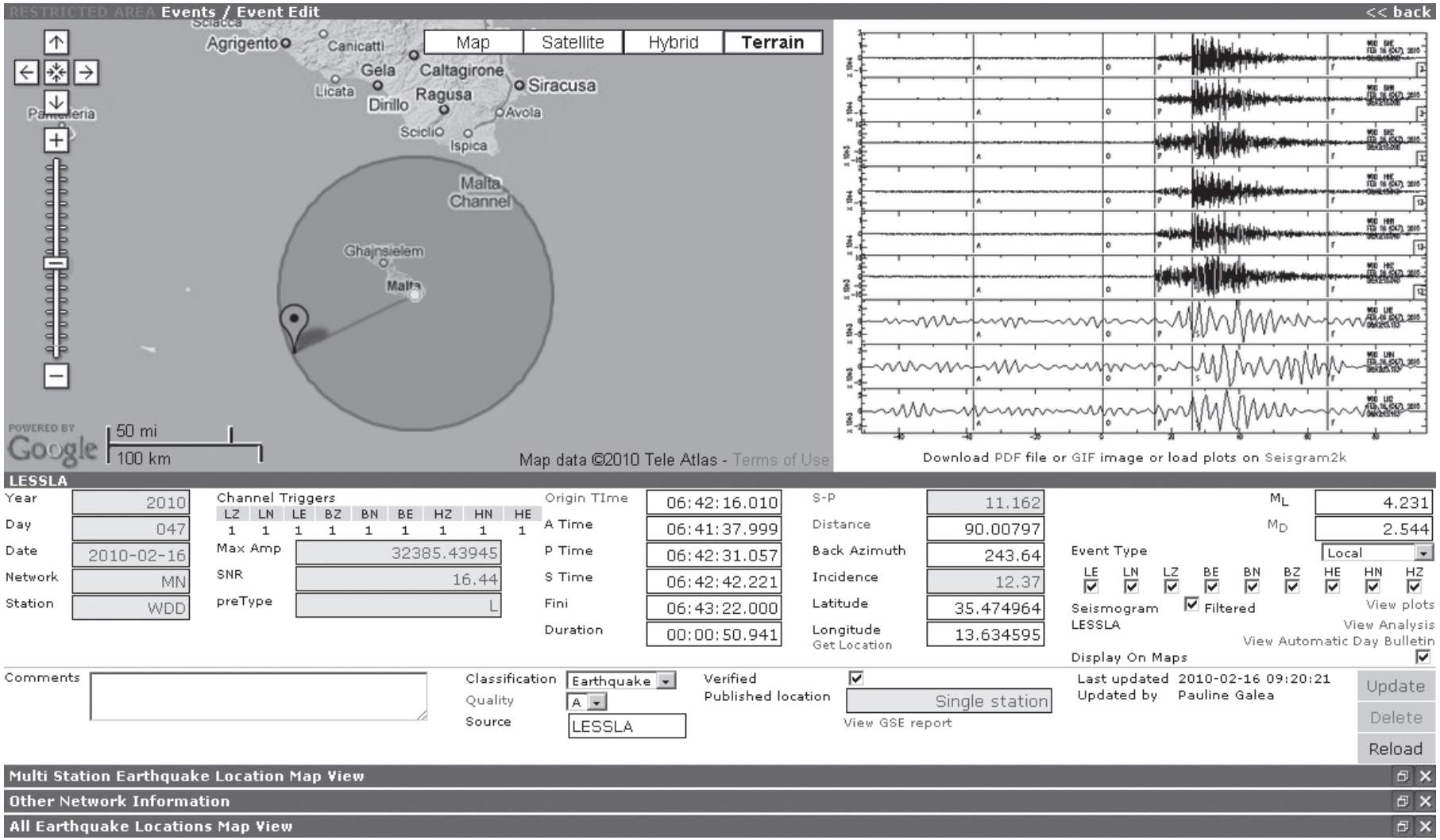

▲ **Figure 8.** The LESSLA Web interface, showing the event analysis window.

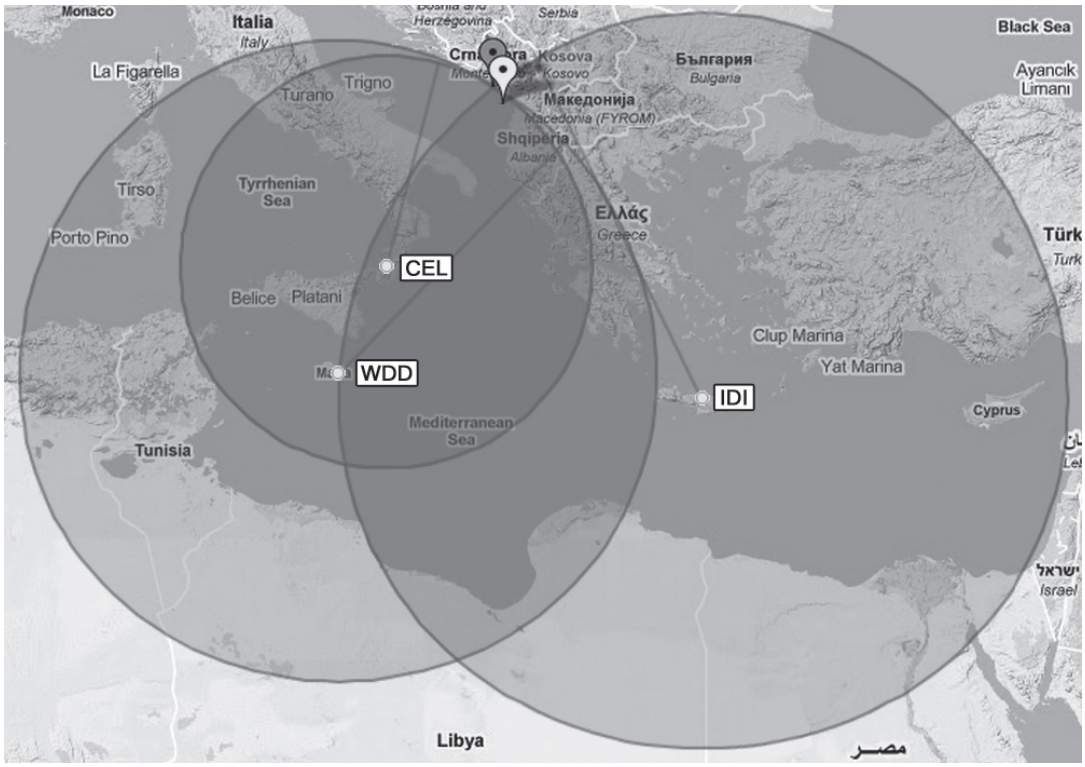

▲ **Figure 9.** Epicenter location using three stations and the "method of circles" (2009/08/21 13:39 M_w 5.0). Dark shaded marker indicates the manually selected earthquake location. Light shaded marker denotes the EMSC location.

LESSLA processes data from other stations and detects earthquake origin times in the database that are within a set time interval from each other (presently set at 15 s to allow for inaccurate pick times), it automatically identifies the recordings as a single event. The system then generates an interactive Google Map, on which the location of the earthquake can be visually and accurately selected as the closest to the intersection of the circles representing distance from each station. An example is shown in Figure 9, where the single-station back-azimuths are not accurate, but the three-station solution is much improved, since the distances are correctly estimated.

RESULTS AND PERFORMANCE

A single-station location method can never be expected to provide the same accuracy as conventional network location methods where good station coverage is available. In particular, it is not the intention of LESSLA to provide accurate epicenter data for seismicity along the well-monitored Hellenic arc or southern Italy, although such activity is routinely detected and located by the system. The motivation behind setting up the present system was chiefly to get a better idea of the extent and magnitude of the seismicity in the Sicily Channel. Nevertheless, it is still instructive to carry out a statistical evaluation of its overall performance.

As regards the triggering mechanism, a three-year evaluation period revealed that the system was triggered 2,995 times, including those events having a trigger weighting less than 11, thus not processed further but listed as "possible events" in the daily report. Of these, 1,024 events were classified as earthquakes or quarry blasts, giving a ratio of false trigger-per-earthquake of approximately 2:1. For events detected within a range of 150 km from WDD, in the Sicily Channel, the minimum magnitude detected was $M_D = 1.14$.

In an evaluation of the picking performance for data from 2006 to 2008, Zammit (2009) found that when 413 events were manually reviewed, 310 (75%) underwent some form of modification to the automatic picks. Of these 310 events, 70% included a modification to the *P* pick, while 47% included a modification to the *S* pick. The parameter that has the largest influence on the accuracy of the location is the back-azimuth, whose accuracy in turn depends on the quality of the signal, particularly the horizontal components, at the *P* onset. When this is high, the system performs very satisfactorily. In the example of Figure 4 (Greece, 2008/02/14 10:09 M_w 6.9), the distance between the two locations, at an epicentral distance of around 650 km from WDD, is only 15 km, implying an azimuth error of less than 2°. The magnitude threshold for the sensitivity of LESSLA obviously increases with increasing distance from WDD. Very small events (duration magnitude less than 2.0) have been reliably located up to epicentral distances of 45 km, provided that the hypocenter is relatively shallow compared to the distance from the station, and that the horizontal component has a strong signal at the start of the first arrivals.

Figure 10A (filled circles) shows earthquakes of magnitude greater than 4.5 that were located by LESSLA, in single-station mode from WDD, as local/regional events during 2006–2009.

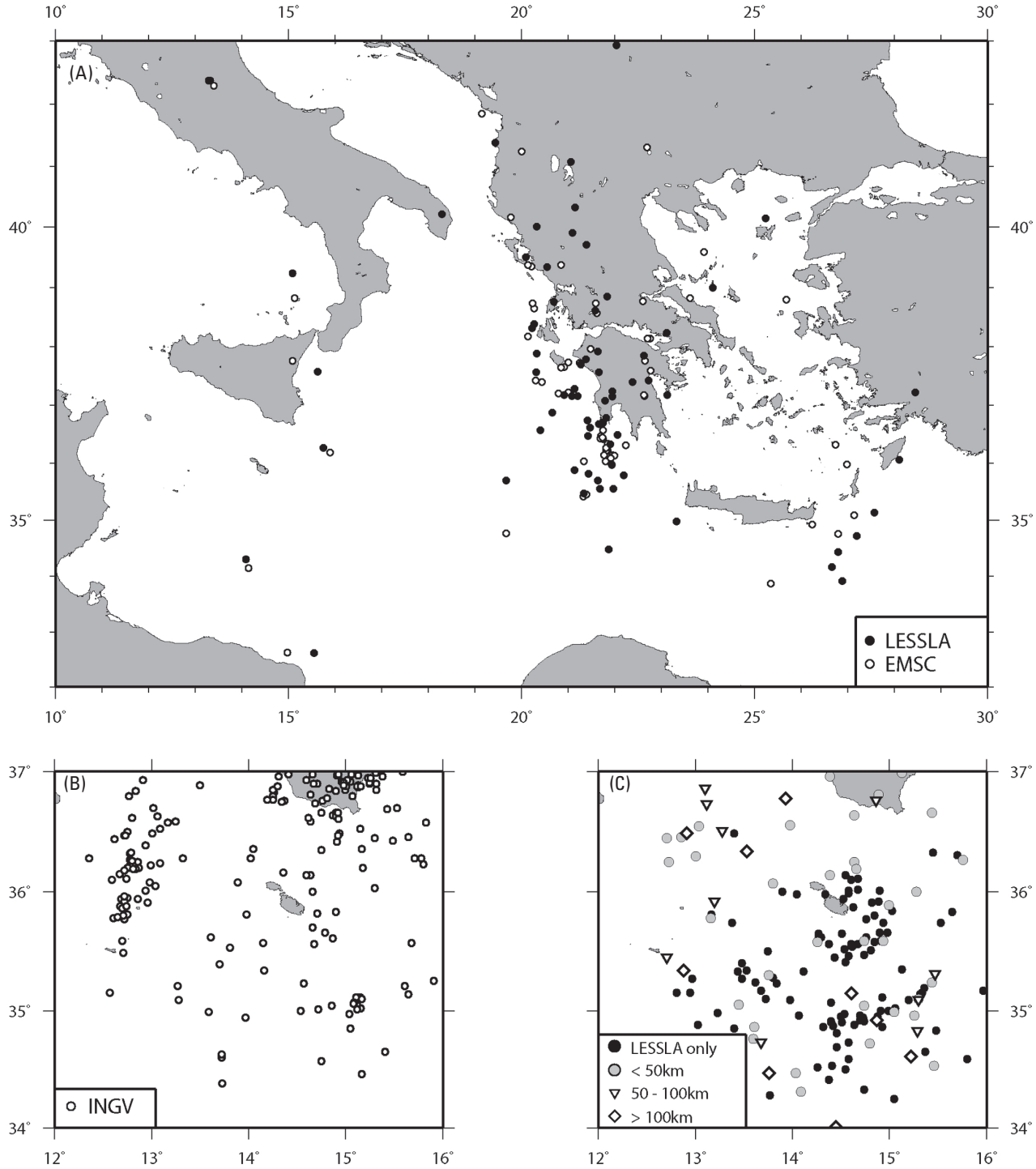

▲ **Figure 10.** A) Manually reviewed LESSLA locations for 2006–2009 (filled circles), magnitude ≥ 4.5, and corresponding EMSC locations for the same events (open circles). B) Events in the INGV bulletin 2006–2009. C) Manually reviewed locations in the Sicily Channel for 2006–2009, indicating the difference in kilometers between LESSLA and INGV locations.

The events shown have undergone manual repicking and relocation when necessary. On the same diagram, the corresponding EMSC locations are shown as open circles. For the closer events, the correspondence between epicenters is seen to be good. The location accuracy clearly suffers as distance increases, as shown by the scatter of epicenters along the Hellenic arc. This arises mostly from the error in back-azimuth calculation. While epicentral distance can be estimated quite accurately, especially after manual processing, an error of, for example, 5° at a distance of 800 km results in an epicentral error of around 70 km. Most epicenters are actually shifted south with respect to the EMSC locations, and it remains to be seen whether this could be due to some geometrical effect related to the propagation of the P_n wave within the subduction zone.

Location accuracy also suffers in proportion to the hypocentral depth. Since LESSLA assumes a surface focus, the radial distance from the station is overestimated in the case of deep events. This is the case with the Tyrrhenian Sea event.

Within the constraints that allow LESSLA to identify and process only local/regional events, the system locates earthquakes with a distance range of around 1,500 km. There appears to be a greater sensitivity of the system toward earthquake activity from the east as opposed to that from the north. Seismicity in Sicily and southern Italy triggers the system much less often than that from the more distant Hellenic arc. This is an observation that has been made a number of times, even with respect to felt earthquakes (*e.g.*, Galea 2007), and most likely reflects a different attenuation regime. In the Hellenic Arc region, the smallest earthquake magnitude detected and measured was M_L 3.1.

In the Sicily Channel, where most of our interest is concentrated, an evaluation of the performance of LESSLA was carried out by comparing our locations with those of INGV, in the cases where the events were located by the latter network. Figure 10B shows the events reported in the INGV bulletin for the Sicily Channel during the period 2006–2009. Figure 10C shows the manually reviewed LESSLA locations of Sicily Channel events for the same period. During this period, around 80 of 190 events located in this region were not reported by INGV or any other network (filled circles). The majority of these events lie to the south of the Maltese islands. The symbol code in the figure gives an indication of the distance between LESSLA and INGV locations. Sixty percent of the events located by both LESSLA and INGV differ by less than 50 km in location. It should be said that for events in the south of the Maltese islands, the network station coverage, especially for small magnitude earthquakes, is very poor, with an azimuthal gap typically exceeding 200°, and therefore the INGV locations themselves are probably also inaccurate. Hence it is difficult to assess the absolute accuracy of the solutions. The two main clusters south of Malta appear to lie along circular arcs centered at WDD. This results partly from the uncertainty in the back-azimuth calculation estimated from WDD, while the distance estimate has a much smaller error after manual verification of the *P* and *S* picks. The seismicity is therefore probably concentrated over a much smaller area.

The difference in epicentral distribution between Figures 10B and 10C is evident. The main feature is the cluster of seismicity to the west of the Maltese islands during this time period, which appears to be very poorly picked up by WDD. This is mainly due to the fact that earthquake signals from this region are often of very poor quality and are too unreliable, especially in terms of back-azimuth calculation, to be included in the epicenter map. This is possibly due to an attenuation effect related to conditions underlying the grabens, and will be discussed in a further publication. It should also be noted that this area, which includes the island station of Pantelleria belonging to the Italian national network, is more favorably surrounded by a seismic network than the south of Malta, and this may have contributed to the increased seismicity detected in this region.

DISCUSSION

A completely automated, self-contained, and flexible system for locating local and regional earthquakes using a single station has been designed, implemented, and tested. The system, LESSLA, has been designed and tailored to suit the particular needs and nature of the WDD broadband station on Malta. It can be applied to any single station; however, proper calibration and optimization of the triggering and weighting parameters must be made. The limitations of a single-station location system, such as LESSLA, are considerable, not least being the instability of the back-azimuth solution at low signal-to-noise ratios and the lack of depth and focal mechanism information obtainable. On the other hand, a large amount of microseismic activity at the periphery of standard land-based seismic networks is probably going undetected and/or unlocated. Such activity may provide useful information about active offshore tectonic processes and may also contribute to seismic hazard studies. Thus, even if accuracy of location may not be as high as desired, the quantitative aspect of earthquake occurrence and the broad delineation of seismically active zones will be enhanced by the addition of such a method to conventional network analysis. The method is particularly relevant to single island stations such as that on Malta. Epicenter location of small events, especially to the south of the Maltese islands could of course be improved by the addition of at least a second station on the islands. Even if this will still not allow for conventional location, it would still provide much tighter constraints on distance and azimuth when the single-station algorithm is run on two stations.

In the case of the Sicily Channel, in which the Maltese islands are situated, the method has proved highly successful in revealing a level of seismicity on the Sicily Channel rift zone that was not previously visible on conventional seismic bulletins. Certain parts of the rift zone have been shown to be more active than others, and the tectonic relevance of these results will be discussed in a separate publication. These findings motivate us to investigate the seismicity further and consider the possibility of more detailed monitoring, possibly by a future ocean bottom seismometer (OBS) experiment, which will be planned according to the indications given by the present study.

ACKNOWLEDGMENTS

This work was supported by a research grant from the University of Malta. We are grateful to an anonymous reviewer for his helpful comments and suggestions for improvement.

REFERENCES

Agius, J. (2003). Discrimination between quarry blasts and microearthquakes around the Maltese Islands. B.Sc. diss., University of Malta, Malta.

Agius, M. R. (2007). Automatic earthquake detection and localisation from a three-component single-station. M.Sc. diss., University of Malta, Malta.

Chen, Z. (2005). A multi-window algorithm for automatic picking of microseismic events on 3-C data, University of Calgary. *Society of Exploration Geophysicists Expanded Abstracts* **24**, 1,288.

Dreger, D. S., and D. V. Helmberger (1990). Broadband modeling of local earthquakes. *Bulletin of the Seismological Society of America* **80**, 1,162–1,179.

Dreger, D. S., and D.V. Helmberger (1993). Determination of source parameters at regional distances with three-component sparse data networks. *Journal of Geophysical Research* **98**, 8,107–8,125.

Frohlich, C., and J. Pulliam (1999). Single-station location of seismic events: A review plea for more research. *Physics of the Earth and Planetary Interiors* **113**, 277–291.

Galea, P. (2007) Seismic history of the Maltese islands and considerations on seismic risk. *Annals of Geophysics* **50**, 725–740.

Illies, J. H. (1981). Graben formation: The Maltese islands, a case history. *Tectonophysics* **73,** 151–168.

Jurkevics, A. (1988). Polarization analysis of three-component array data. *Bulletin of the Seismological Society of America* **78**, 1,725–1,743.

Kanasewich, E. R. (1981). *Time Sequence Analysis in Geophysics*. Edmonton: University of Alberta Press.

Kim, S. G., and F. C. Gao (1997). Study on some characteristics of earthquakes and explosions using the polarization method. *Journal of Physics of the Earth* **45**, 13–27.

Lockmann, A. B., and R. M. Allen (2005). Single-station Earthquake Characterization for Early Warning. *Bulletin of the Seismological Society of America* **95**, 2,029–2,039.

MacBeth, C., and H. Dai (1996). Arrival type identification in local earthquake data using an artificial neural network. *Cahiers du Centre Européen de Géodynamique et de Séismologie* **12**, 169–178.

Magotra, N., N. Ahmed, and E. Chael (1987). Seismic event detection and source location using single-station (three-component) data. *Bulletin of the Seismological Society of America* 77, 958–971.

Park, J., F. L. Vernon, and C. R. Lindberg (1987). Frequency dependent polarization analysis of high-frequency seismograms. *Journal of Geophysical Research* **92**, 12,664–12,674.

Reuther, C.-D., and G. H. Eisbacher (1985). Pantelleria Rift—crustal extension in a convergent intraplate setting. *Geologische Rundschau*. **74**, 585–597.

Roberts, R. G., A. Christoffersson, and F. Cassidy (1989). Real-time event detection, phase identification and source location estimation using single station three-component seismic data. *Geophysical Journal International* **97**, 471–480.

Ruud, B. O., E. S. Husebye, S. F. Ingate, and A. Christofferson (1988). Event location at any distance using seismic data from a single, three-component station. *Bulletin of the Seismological Society of America* **78**, 308–325.

Ruud, B. O., and E. S. Husebye (1992). A new three-component detector and automatic single-station bulletin production. *Bulletin of the Seismological Society of America* **82**, 221–237.

van Eck, T., C. Trabant, B. Dost, W. Hanka, and D. Giardini (2004). Setting up a virtual broadband seismograph network across Europe. *Eos, Transactions, American Geophysical Union* **85** (13); doi:10.1029/2004EO130001.

Zammit, D. (2009). A performance evaluation of a single-station earthquake location algorithm (LESSLA) implemented at WDD seismic station. B.Sc. diss., University of Malta, Malta.

Zhao, L.-S., and D.V. Helmberger (1991). Broadband modeling along a regional shield path, Harvard recording of the Saguenay earthquake. *Geophysical Journal International* **105**, 301–312.

Zhizhin, M. N., D. Rouland, J. Bonnin, A. D. Gvishiani, and A. Burtsev (2006). Rapid estimation of earthquake source parameters from pattern analysis of waveforms recorded at a single three-component broadband station, Port Vila, Vanuatu. *Bulletin of the Seismological Society of America* **96**, 2,329–2,347.

Physics Department
University of Malta
Msida MSD2080
Malta
pauline.galea@um.edu.mt
(P. G.)